

Electronic Supplementary Information

Effects of Ultraviolet Light on Silver Nanoparticle Mobility and Dissolution

Anjuliee M. Mittelman¹, John D. Fortner², and Kurt D. Pennell^{1,}*

¹Department of Civil and Environmental Engineering, Tufts University, 200 College Ave,
Medford, Massachusetts, 02155, USA

²Department of Energy, Environmental, and Chemical Engineering, Washington University at St.
Louis, 1 Brookings Drive, St. Louis, Missouri, 63130, USA

Corresponding Author: Kurt D. Pennell

[Email: kurt.pennell@tufts.edu](mailto:kurt.pennell@tufts.edu); Fax: +1 (617) 627 3994; Tel: +1 (617) 627 3099

Number of pages: 11

Number of figures: 9

Number of tables: 1

1. Transmission Electron Micrographs

Transmission electron microscopy (TEM) was used to collect images of UVB-aged nAg following a 3-day light exposure. Images show evidence of aggregate formation following aging (Fig. S1).

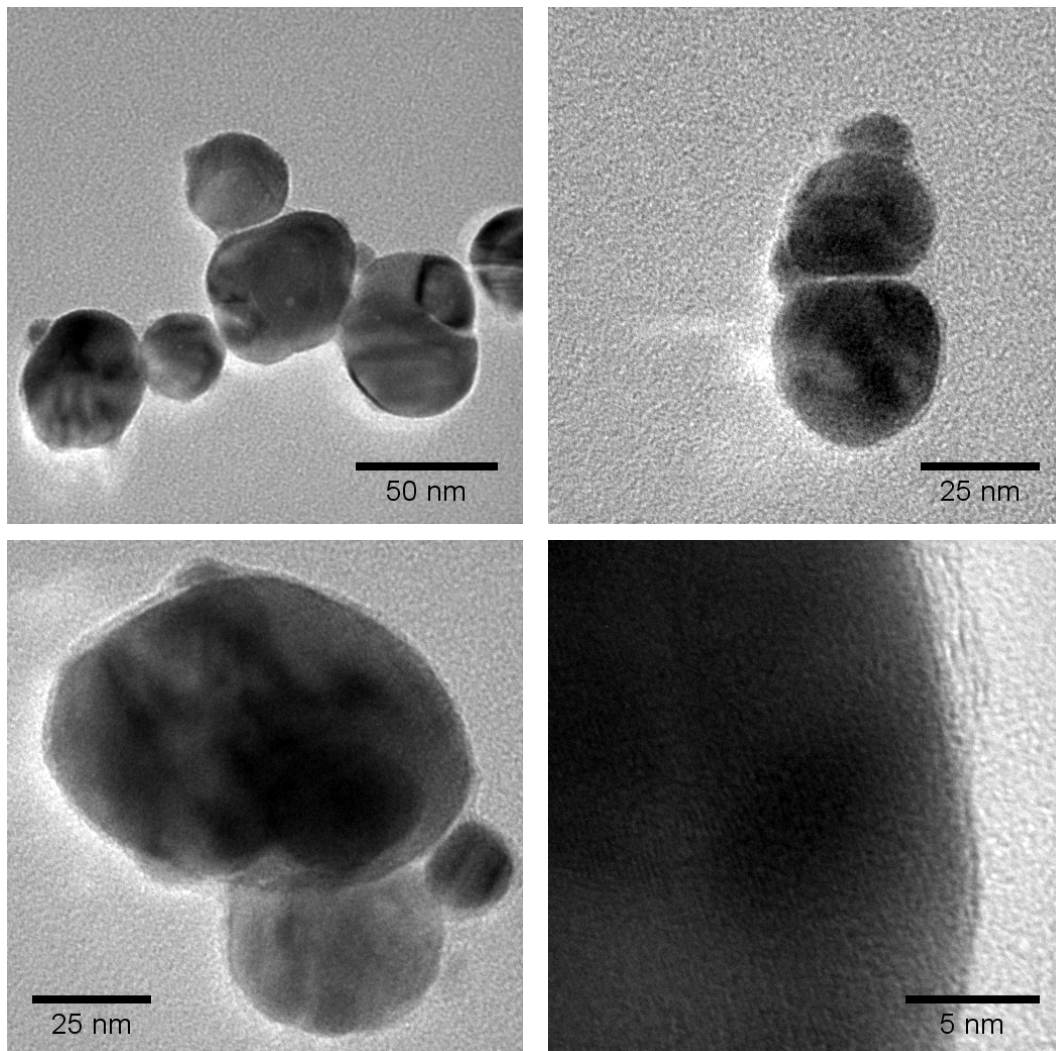


Fig. S1 Transmission electron micrographs of 3-day UVB-aged nAg

2. Attachment Efficiency of Fresh and UV-aged nAg

Reaction-limited aggregation kinetic parameters were derived from the initial rate of increase in the hydrodynamic diameter (D) using the approach of Chen and Elimelech.¹ The increase in particle diameter is linearly dependent on the primary particle concentration, N_0 , as well as the initial aggregation rate constant, k_1 .

$$\left. \frac{dD(t)}{dt} \right|_{t \rightarrow 0} \propto k_1 N_0 \quad (1)$$

The initial rate, k_1 , is obtained from the initial slope (D vs. t) up to a point in time when the radius reaches a prescribed value (e.g., $1.5D_0$). The CCC is the point where aggregation kinetics transition from a rate-limited to a diffusion-limited regime, or the point at which the aggregation rate becomes independent of ionic strength.¹ The aggregation attachment efficiency (α_A) (also referred to as the inverse stability ratio, $1/W$) is calculated for different electrolyte concentrations by normalizing slopes obtained under different solution chemistry to the slope obtained under fast aggregation conditions.¹

$$\alpha_A = \frac{1}{W} = \frac{k_1}{k_{1,fast}} = \frac{\frac{1}{N_0} \left. \frac{dD(t)}{dt} \right|_{t \rightarrow 0}}{\frac{1}{(N_0)_{fast}} \left. \frac{dD(t)}{dt} \right|_{t \rightarrow 0, fast}} \quad (2)$$

Aggregation kinetic studies were conducted with fresh and UV-aged nAg at NaNO_3 concentrations of 5-300 mM. Fresh nAg were stable in NaNO_3 solutions up to 40 mM, while UVA and UVB-aged nAg began to aggregate at 5-10 mM (data not shown). Attachment efficiency as a function of ionic strength is shown for fresh and 3d-aged nAg in Fig. S2. Kinetic data were used to determine the critical coagulation concentration (CCC) for each system (Table S1).

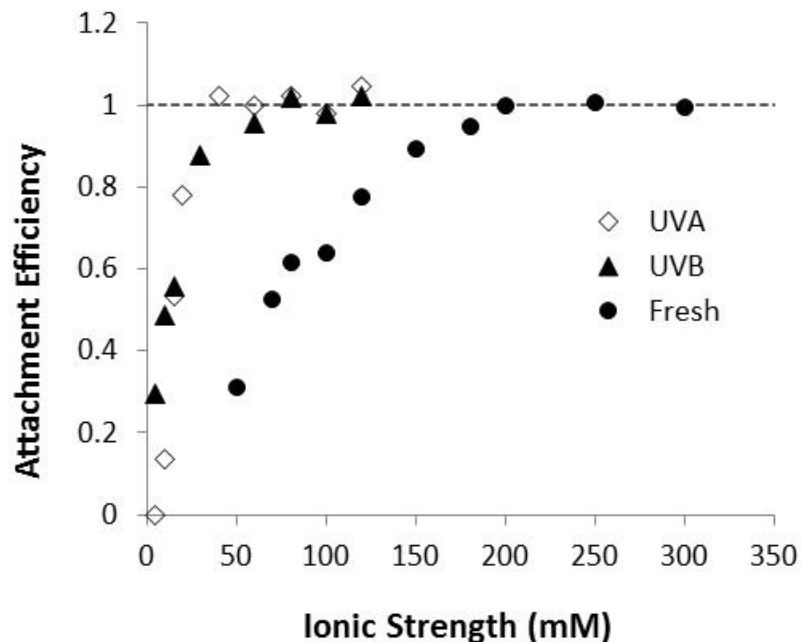


Fig. S2 Attachment efficiency as a function of ionic strength for fresh and UV-aged nAg following a 3 day exposure.

Table S1 Critical coagulation concentration (CCC) for fresh and UVA- and UVB-aged nAg as a function of exposure time.

| Aging Time (d) | Fresh (mM) | UVA (mM) | UVB (mM) |
|----------------|------------|----------|----------|
| 1 | 161.4 | 37.8 | 21.4 |
| 3 | 182.4 | 25.5 | 15.1 |
| 7 | 175.9 | 23.8 | 34.8 |

3. Surface Plasmon Resonance during UV Exposure

UV exposure resulted in changes in the UV-vis spectra of nAg suspensions (Fig. S3). In UVA-aged suspensions, a significant red shift (395 nm to 401 nm) occurred between 0 and 24 hr of aging and spectra became broader over time. Peak height remained constant during the first 4

days and then gradually decreased between days 5 and 7. In UVB-aged nAg suspensions, peak height decreased at each successive time point and spectra also red-shifted during the first 24 h (ca. 396 to 403 nm). Red shifts, broadening of spectra, and decreases in surface plasmon resonance are indicative of surface oxidation and aggregation, consistent with previous observations.²⁻⁶

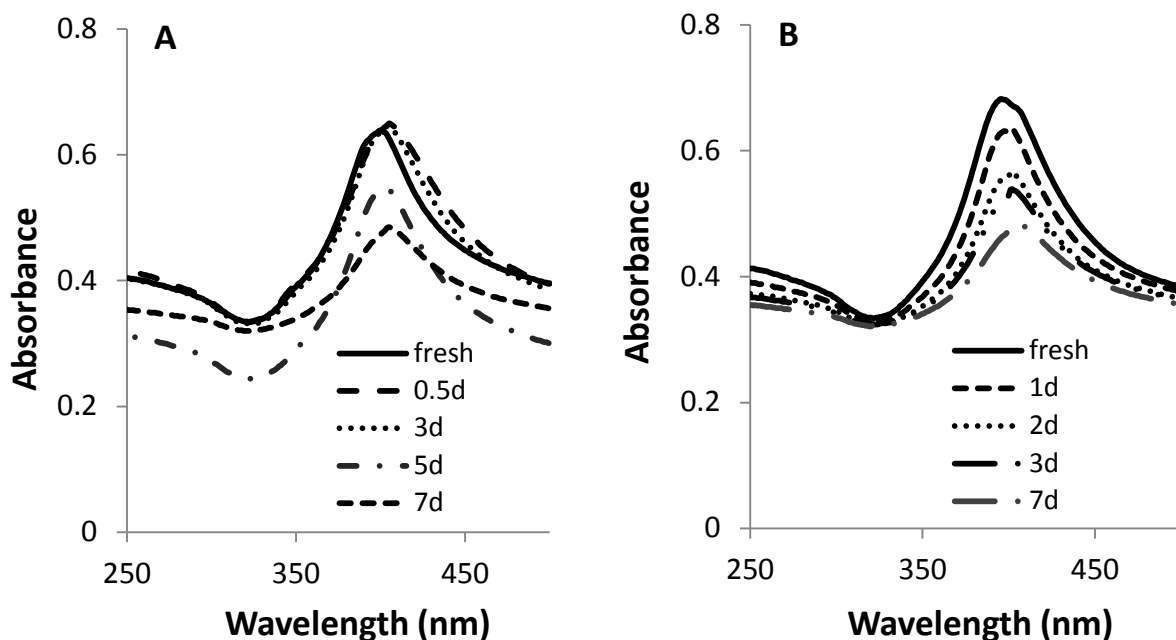


Fig. S3 UV-vis spectra of nAg in DI water during exposure to (A) UVA light and (B) UVB light.

4. Characterization of 3-day UV-aged nAg in Electrolyte Solutions

Prior to conducting column experiments, batch reactors studies were conducted to monitor the mean diameter (Fig. S4A), zeta potential (Fig. S4B), and dissolution kinetics (Fig. S5) of 3-day UV-aged nAg for 180 min in 10 mM and 20 mM NaNO₃ solutions. The x-axis represents time elapsed after NaNO₃ addition to suspensions containing 3-day UV-aged nAg.

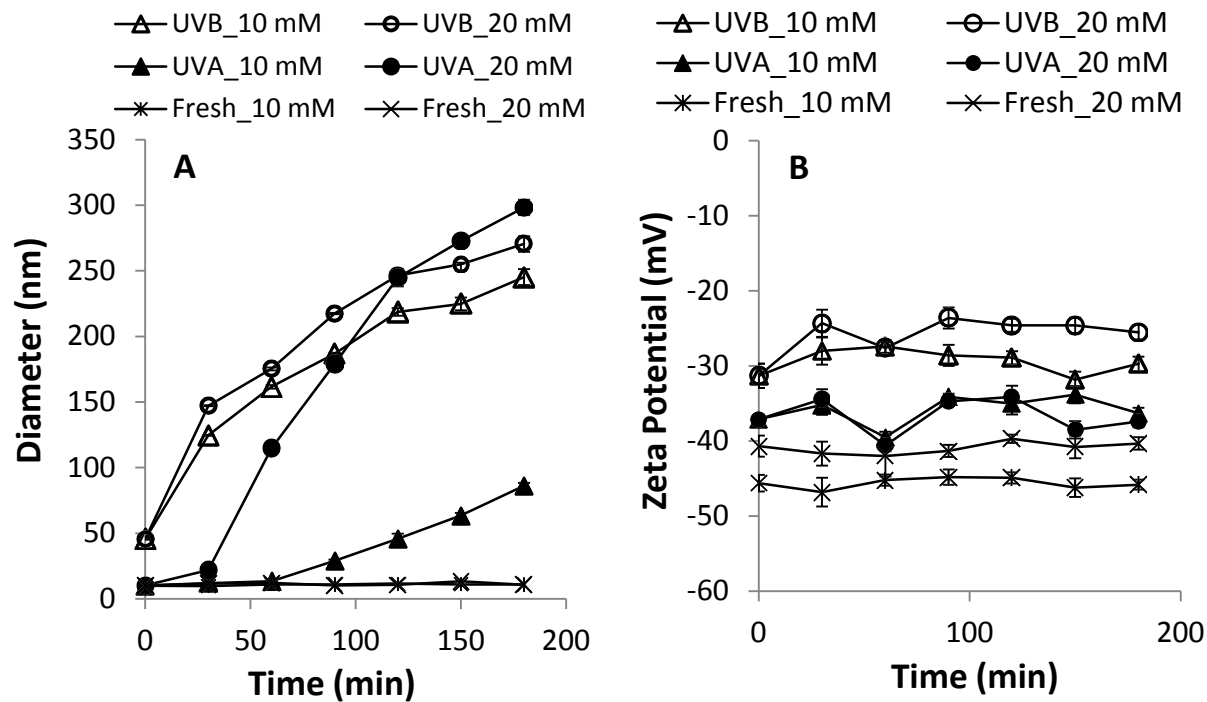


Fig. S4 Change in (A) size and (B) zeta potential of 3-day UV-aged nAg in 10 mM and 20 mM NaNO₃ solutions.

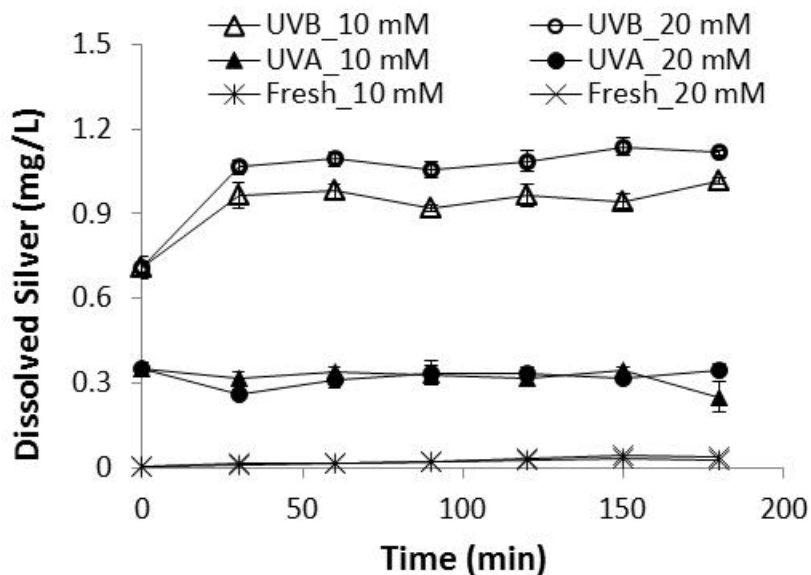


Fig. S5 Ag⁺ release from 3-day UV-aged nAg in 10 mM and 20 mM NaNO₃ solutions.

5. Free Radicals and Surface Aging

A set of batch experiments was conducted with the hydroxyl radical scavenger tert-butyl alcohol (tBOH) in order to determine the role of free radicals in UV aging of nAg. Batch reactors containing nAg and 15 mM tBOH were exposed to UV light for 7 days and monitored daily for changes in mean diameter, zeta potential, and Ag⁺ release. The presence of tBOH was found to reduce aggregation of nAg by up to 50% (Fig. S6) and reduce the magnitude of changes in zeta potential by ca. 60% (Fig. S7). tBOH also reduced Ag⁺ release by 3-6 fold compared with tBOH-free suspensions (Fig. S8). These findings indicate that free radicals, particularly OH[•], are largely responsible for the surface degradation of citrate-coated nAg observed during UV light exposure.

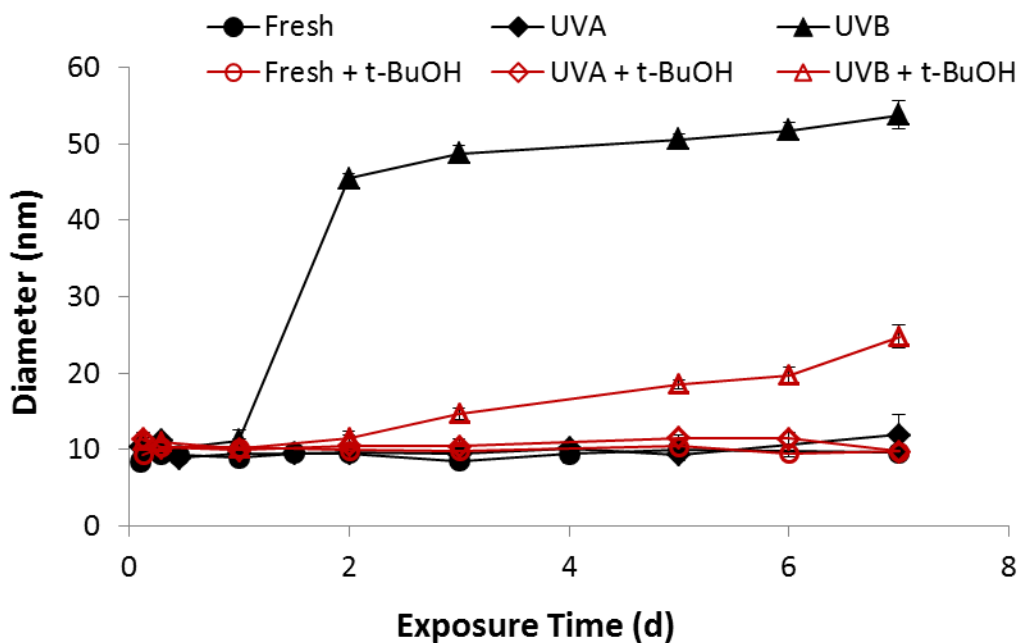


Fig. S6 Change in mean diameter of nAg suspensions with and without 15 mM t-BuOH exposed to UVA and UVB light for 7 days in a photoreactor.

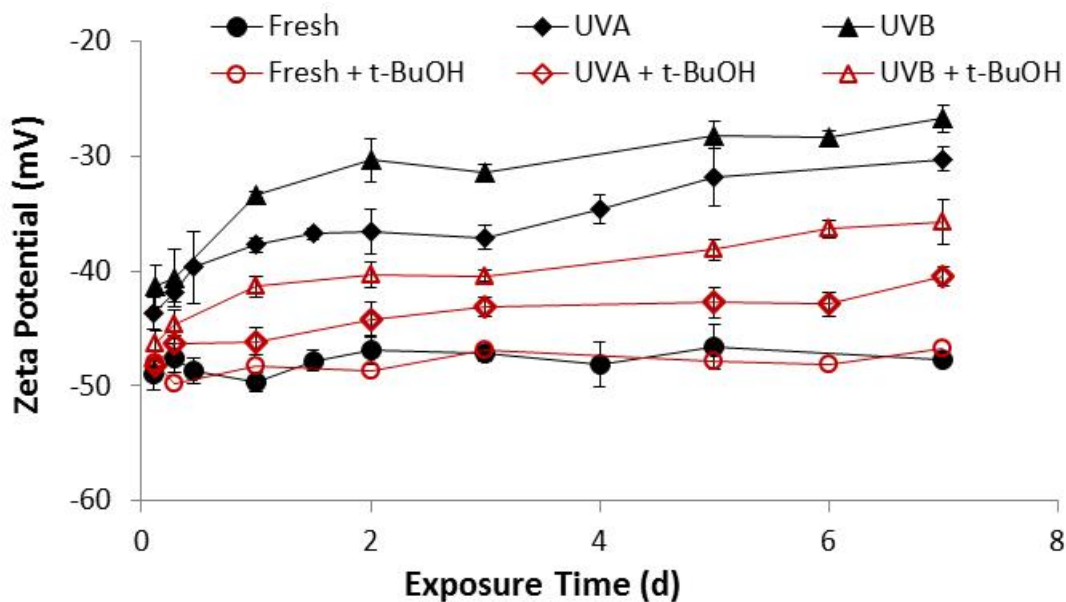


Fig. S7 Change in zeta potential of nAg suspensions with and without 15 mM t-BuOH exposed to UVA and UVB light for 7 days in a photoreactor.

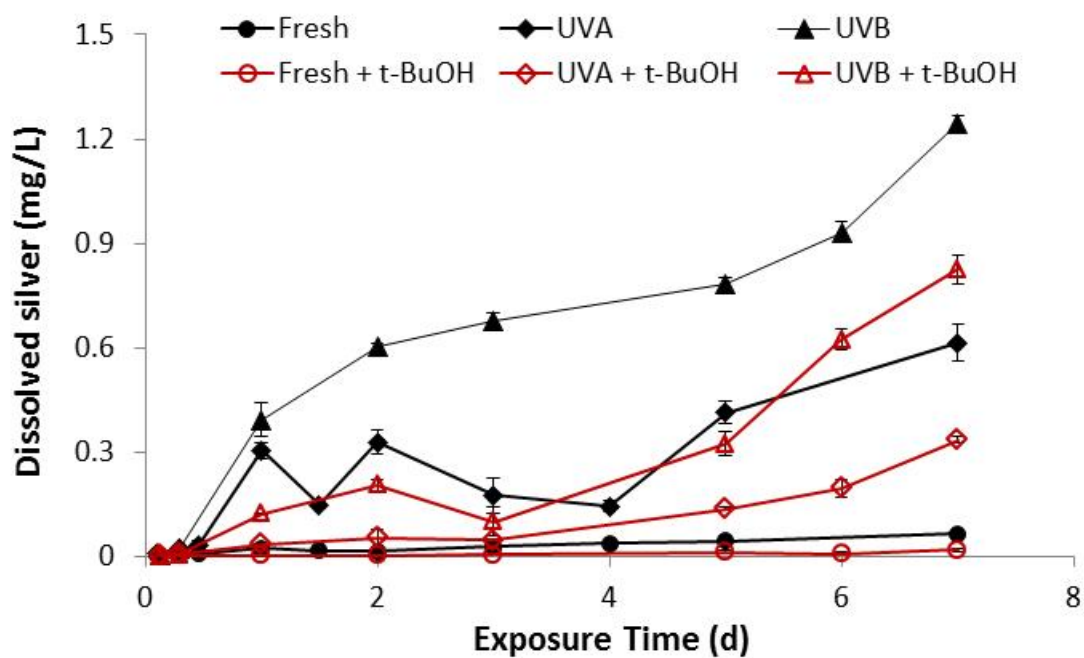


Fig. S8 Ag⁺ release from nAg with and without 15 mM t-BuOH exposed to UVA and UVB light for 7 days in a photoreactor.

6. nAg Retention Profiles

Retention profiles were generated for each column experiment by analyzing the solid-phase silver concentration along the length of the column. Retention data for fresh and UV-aged nAg at 10 mM NaNO₃, fresh and UV-aged nAg at 20 mM NaNO₃, and UVA-aged nAg at different flow rates are shown in Fig. S9 as graphs A, B, and C, respectively. Retention profiles from experiments with both fresh and UV-aged nAg were hyper-exponential in shape, with the highest deposition measured within a distance of 2-3 cm from the column inlet. These observations are consistent with hyper-exponential profiles reported previously in column studies with nAg⁷ and other nanoparticle systems.⁸⁻¹⁰ UVB-aged nAg exhibited lower breakthrough (greater retention) compared with UVA-aged nAg, but dissolved more rapidly resulting in lower overall retention.

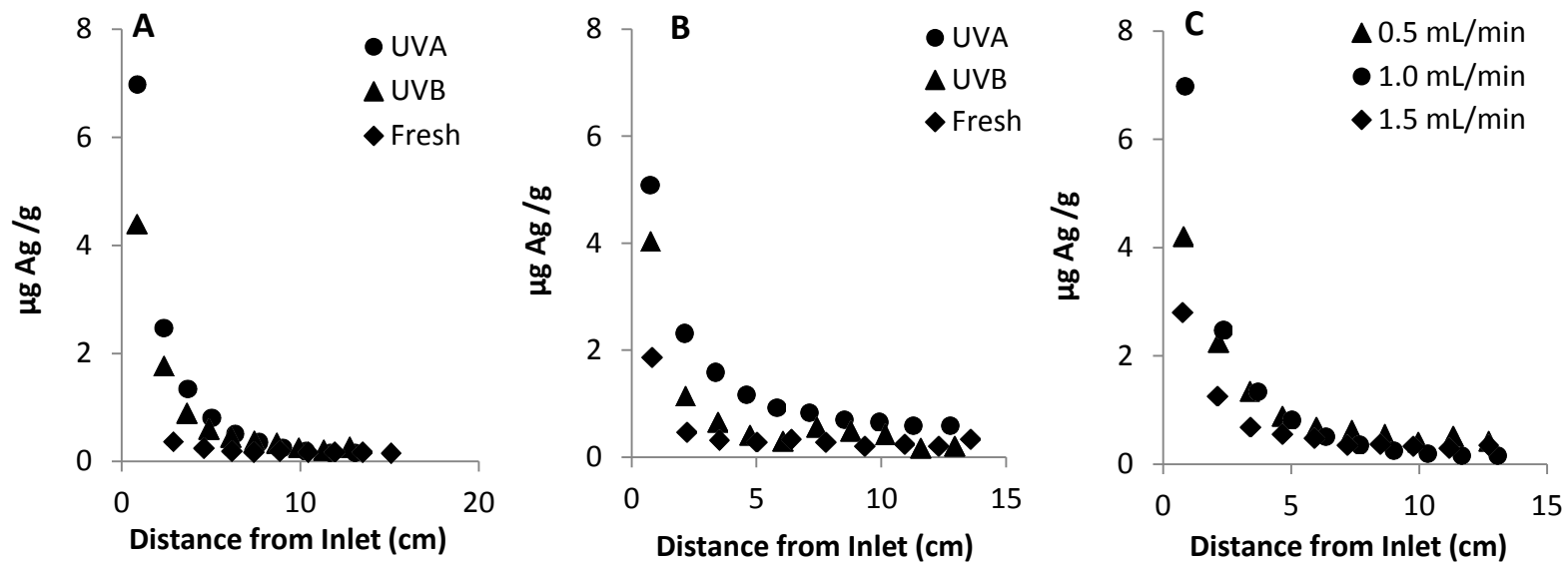


Fig. S9 Retention profiles for fresh and UV-aged nAg columns (1.0 mL/min) conditioned with (A) 10 mM NaNO_3 and (B) 20 mM NaNO_3 , and (C) for UVA-aged columns as a function of flow rate in 10 mM NaNO_3 .

References

- 1 K. L. Chen and M. Elimelech, *Langmuir*, 2006, **117**, 10994–11001.
- 2 A. Henglein, *Anal. Chem.*, 1998, **2**, 444–450.
- 3 M. Chen, L.-Y. Wang, J.-T. Han, J.-Y. Zhang, Z.-Y. Li and D.-J. Qian, *J. Phys. Chem. B*, 2006, **110**, 11224–31.
- 4 X. Li, J. J. Lenhart and H. W. Walker, *Langmuir*, 2010, **26**, 16690–8.
- 5 X. Li and J. J. Lenhart, *Environ. Sci. Technol.*, 2012, **46**, 5378–86.
- 6 Y. Cheng, L. Yin, S. Lin, M. Wiesner, E. Bernhardt and J. Liu, *J. Phys. Chem. C*, 2011, **115**, 4425–4432.
- 7 Y. Liang, S. a Bradford, J. Šimunek, H. Vereecken and E. Klumpp, *Water Res.*, 2013, **47**, 2572–82.
- 8 I. Chowdhury, Y. Hong, R. J. Honda and S. L. Walker, *J. Colloid Interf. Sci.*, 2011, **360**, 548–55.
- 9 X. Jiang, M. Tong, H. Li and K. Yang, *J. Colloid Interf. Sci.*, 2010, **350**, 427–434.
- 10 D. Kasel, S. A. Bradford, J. Šimunek, M. Heggen, H. Vereecken and E. Klumpp, *Water Res.*, 2013, **47**, 933–44.